

New Phenyl-Substituted PPV Derivatives for Polymer Light-emitting Diodes—Synthesis, Characterization and Structure–Property Relationship Study

Zhi-Kuan Chen,* Nancy Hoi Sim Lee, and Wei Huang

Institute of Materials Research and Engineering (IMRE), 3 Research Link, Singapore 117602, Republic of Singapore

Yi-She Xu and Yong Cao

Institute of Polymer Optoelectronic Materials and Devices, South China University of Technology, Guangzhou 510640, People's Republic of China

Received July 29, 2002; Revised Manuscript Received January 3, 2003

ABSTRACT: Three new PPV derivatives with dialkoxyphenyl substituents, **BEH2P–PPV**, **BEH3P–PPV**, and **BEH4P–PPV** have been synthesized. The polymers were characterized by FT-IR, ¹H NMR, and elemental analysis. The polymers possess excellent solubility, high molecular weights, high photoluminescence efficiencies and good thermal stability. The influence of substitution pattern on the formation of structural defects has been investigated by measuring the signal due to tolane–bisbenzyl moieties (TBB) in the proton NMR spectra. **BEH2P–PPV** with a steric phenyl group at the ortho-position on the side phenyl ring shows the lowest amount of TBB, which indicates suitable steric hindrance can be applied to suppress the formation of irregular head-to-head and tail-to-tail linkage in the polymer chains. In addition, the polarity of solvents used for the Gilch polymerization will also affect the amount of irregular structure in the polymers. Polar solvents such as THF will result in polymers with low TBB content. Energy level measurement from cyclic voltammetry revealed that the influences of the substitution pattern on the HOMOs and LUMOs are different. The three polymers possess similar HOMO energy levels while the LUMO of **BEH4P–PPV** is much higher than that of the other two polymers. Polymer light-emitting diodes fabricated from **BEH2P–PPV**, **BEH3P–PPV**, and **BEH4P–PPV** with the configuration of ITO/PEDOT/polymer/Ba/Al, emitted bright blue-green to green light with the maximum peaks at 496, 488, and 525 nm, respectively. The turn-on electric field and maximum external quantum efficiencies of the diodes are 0.30, 0.50, and 0.42 MV/cm and 0.37%, 0.66%, and 0.25% respectively. The quantum efficiency is mainly determined by the electron injection from the cathode. With the highest luminance, lowest turn-on electric field, and good quantum efficiency as well as negligible structural defects, **BEH2P–PPV** is the most promising material among the three polymers for polymer light-emitting diodes.

Introduction

Polymeric light-emitting diodes (PLEDs) have attracted significant attention from both the academic community and industry since the first report of the PLED device fabricated from poly(*p*-phenylenevinylene) (PPV) in 1990,¹ because of their potential application for large-area flat panel displays with the advantages of low cost, wide viewing angle, fast switching time, high efficiency, and low driving voltage.^{2–6} Ever since, remarkable progress has been made on the performance of PLEDs, which has triggered a strong motivation to commercialize this technology in displays. However, there are a number of issues that need to be resolved, for example, low electroluminescent efficiencies, short operational lifetime, and luminescent stability. The low quantum yields are attributed to three main reasons. The first reason is the imbalance of hole/electron injection and transport in the emission layer in devices because most of the emissive polymers conduct holes in preference to electrons. This situation can largely be improved by introducing electron-deficient moieties into the polymer backbone or as the side chains^{7–9} or by optimizing device configurations through adding charge

injection/transporting layers between the light-emitting polymer film and electrodes to balance the charge carriers.^{10,11} The second reason for low quantum efficiencies in the solid state is because of interchain interactions such as aggregation and excimer formation, which will lead to a self-quenching process of excitons.^{12–15} The effective strategy to suppress this drawback is to introduce asymmetric structure or bulky substitution to prevent close packing of the polymer chains with each other.^{16–22} The third main factor that limits the quantum efficiency is the presence of defects in the polymer where excitons will be trapped and nonradiative decay will occur. In addition to reducing quantum efficiency, it is believed that polymer structural defects are also responsible for the short operational lifetime of LED devices²³ which may be attributed to accelerated degradation of polymers initiated by the defects. Compared to the first two issues, to overcome this obstacle is a bigger challenge. It requires a deeper understanding of the polymerization mechanism and careful control of polymerization conditions and also the need for systematic investigation of the structure–property relationship of light-emitting polymers.

PPV and its derivatives have been intensively investigated since 1990. Today, they are still one of the most valuable and frequently used light-emitting materials

* Corresponding author: Telephone: +65-6874 4331. Fax +65-6872 0785. E-mail: zk-chen@imre.a-star.edu.sg.

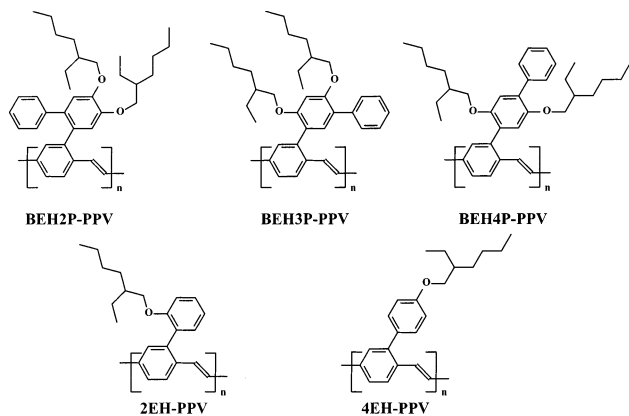


Figure 1. Chemical structures of the dialkoxy-substituted PPVs and model polymers.

because of their good processability, structural diversity, thermal stability, good mechanical property and high luminescence. PPVs are normally synthesized by two methods: precursor route and direct solution polymerization for organic soluble polymers. Several synthetic approaches for soluble polymers have been established including, dehydrohalogenation (Gilch route), Wittig–Horner reaction, Heck and Suzuki reaction, and so on. Among the methods investigated, the Gilch procedure is very simple and can normally result in polymers with high molecular weights, narrow polydispersity indices and high structural regularity. A few PPV derivatives such as MEH–PPV, OC₁C₁₀–PPV, and phenyl-substituted PPVs (Ph–PPVs, reported by COVION) with such promising properties have been successfully prepared through the Gilch route.^{23–25} However, through COVION's research, it was found that there are a large amount of defects in both alkoxy-substituted PPVs and phenyl-substituted PPVs, especially in the latter ones, which are not related to the primary structure.^{23,26} The main irregularity in the PPVs is identified to be toluene–bisbenzyl moieties (TBB), which are formed due to head-to-head and tail-to-tail linkage during polymerization. They have also demonstrated that there is an obvious correlation between the number of structural defects and the luminance efficiency and lifetime of the corresponding devices. To address this problem, a research group in COVION found that introducing an electron-donating methoxy group into the phenyl-substituted monomer can result in a largely improved regular structure. On the basis of this monomer, a few copolymers have been prepared with very good device performance with regards to the efficiency and device lifetime. However, this approach has only partially solved the limitation caused by structural defects in PPVs. Green-light-emitting PPVs (without the strong electron-donating groups in the monomer) with satisfactory operational stability are still not available. Therefore, further effort devoted to PPVs to seek effective ways to control or even completely suppress the formation of structural defects is essential for development of commercially valuable light-emitting polymers, especially green-light-emitting polymers.

In this paper, we report the synthesis, characterization, and electroluminescent properties of a series of dialkoxy phenyl-substituted PPV derivatives. The structures of the polymers are displayed in Figure 1. The polymers in this paper, **BEH2P–PPV**, **BEH3P–PPV**, and **BEH4P–PPV**, possess dialkoxy-branched long

chains in the side chain in order to improve solubility in common organic solvents, as well as to minimize interchain interactions and thus achieve high photoluminescence quantum efficiencies. Additional phenyl rings incorporated into the polymer side chains were designed to allow us to investigate the steric effect on the formation of structural defects as well as to improve the thermal stability of the polymers. In addition, model compounds **2EH–PPV** and **4EH–PPV** have also been synthesized to study (i) solvent effects and (ii) substitution effects on polymerization and the number of structural defects in the polymers. To the best of our knowledge, although a few solvents have been exploited for the Gilch route polymerization, no effort on this issue has been reported.

Experimental Section

Nuclear magnetic resonance (NMR) spectra were collected on a Bruker ACF 300 spectrometer using chloroform-*d* as a solvent and tetramethylsilane (TMS) as an internal standard. Electron-impact mass spectra were obtained from a Micromass VG7035F mass spectrometer using an ion current of 70 eV. Fourier transform infrared (FT-IR) spectra were recorded on a Bio-Rad FTS 165 spectrometer by dispersing samples in KBr disks. Ultraviolet–visible (UV–vis) and fluorescence spectra were obtained using a Shimadzu UV 3101PC UV–vis–NIR spectrophotometer and a Perkin-Elmer LS 50B luminescence spectrometer with a xenon lamp as light source, respectively. Elemental analyses were performed on a Perkin-Elmer 2400 elemental analyzer for C, H, Cl, and Br determination. Thermogravimetric analyses (TGA) were conducted on a Du Pont Thermal Analyst 2100 system with a TGA 2950 thermogravimetric analyzer under a heating rate of 20 °C/min and a nitrogen flow rate of 70 cm³/min. Cyclic voltammetry measurements were taken on an EG&G Parc model 273A potentiostat/galvanostat under argon atmosphere. All potentials were measured against a Ag/Ag⁺ (0.10 M AgNO₃ in acetonitrile) electrode (0.34 V vs SCE), and all experimental values were corrected with respect to SCE. GPC analysis was conducted on Waters 2690 Separation Module equipped with a Waters 410 differential refractometer HPLC system and Waters Styragel HR3, HR4, and HR5 columns in series using polystyrene as a standard and THF as eluent.

LED Devices. Polymers were dissolved in chloroform and filtered through a 0.45 μm PTFE filter. Patterned indium tin oxide (ITO) coated glass substrates were cleaned with acetone, detergent, and distilled water sequentially in an ultrasonic bath. After treatment with oxygen plasma, 1500 Å of poly(3,4-ethylenedioxythiophene) (PEDOT) doped with poly(styrenesulfonic acid) (PSS) (Batron-P 4083, Bayer AG) was spin-coated onto the substrate followed by drying in a vacuum oven at 80 °C for 8 h. A thin film of polymer was coated onto the anode by spin casting inside a drybox. The film thickness of the active layers was around 80 nm, as measured with a Tencor Alfa step 500 surface profiler (Oriel). Ba and Al layers were vacuum-evaporated on top of an EL polymer under a vacuum of 1 × 10⁻⁴ Pa. Device performances were measured inside a drybox. Current–voltage (*I*–*V*) characteristics were recorded with a Keithley 236 source meter. EL spectra were recorded by Oriel INTASPEC IV CCD Spectrograph. Luminescence and external quantum efficiencies were determined by a calibrated photodiode.

Synthesis of model polymers 2EH–PPV and 4EH–PPV. The monomers for **2EH–PPV** and **4EH–PPV** were synthesized according to the procedure described for poly[2-(4'-decyloxyphenyl)-1,4-phenylenevinylene].²⁷

Synthesis of Poly[2-(2'-(2''-ethylhexyloxy)phenyl)-1,4-phenylenevinylene] (2EH–PPV). A solution of 1,4-bis-(chloromethyl)-2-(2'-(2''-ethylhexyloxy)phenyl)benzene (0.20 g, 0.53 mmol) in 10 mL of anhydrous THF was added a solution of 1 M potassium *tert*-butoxide (3.2 mL) in 25 mL of anhydrous THF at room temperature with stirring for 24 h. An orange

polymer (75 mg) was obtained in 46% yield. FT-IR (cm^{-1}): 3057, 3024, 2923, 2856, 1598, 1445, 1380, 1235, 1108, 1028, 960, 895, 820, 749, 631, 471. ^1H NMR (ppm) (300 MHz, CDCl_3): δ 7.70–7.00 (aromatic, 9H), 3.75 (2H), 1.53 (1H), 1.26–1.08 (8H), 0.70 (6H). Anal. Calcd for $\text{C}_{22}\text{H}_{26}\text{O}$: C, 86.27; H, 8.50. Found: C, 84.09; H, 8.41.

Synthesis of Poly[2-(4'-(2''-ethylhexyloxy)phenyl)-1,4-phenylenevinylene] (4EH-PPV). 4EH-PPV was synthesized according to the procedure described for 2EH-PPV using 1,4-bis(chloromethyl)-2-(4'-(2''-ethylhexyloxy)phenyl)benzene (0.22 g, 0.59 mmol) in 10 mL of anhydrous THF and 1 M potassium *tert*-butoxide (3.5 mL) in 25 mL of anhydrous THF. An orange polymer (84 mg) was obtained in 47% yield. FT-IR (cm^{-1}): 3038, 2956, 2925, 2850, 1607, 1511, 1492, 1464, 1240, 1174, 1110, 1027, 961, 830, 617. ^1H NMR (ppm) (300 MHz, CDCl_3): δ 7.70–7.00 (aromatic, 9H), 3.90 (2H), 1.76 (1H), 1.50–1.35 (8H), 0.92 (6H). Anal. Calcd for $\text{C}_{22}\text{H}_{26}\text{O}$: C, 86.27; H, 8.50. Found: C, 84.29; H, 8.25.

The influence of solvent on the structural defects was studied using 1,4-dioxane and *p*-xylene as a polymerization solvent for 4EH-PPV while keeping all other conditions the same.

Synthesis of DialkoxyphenylSubstituted PPVs. Synthesis of 1,2-Bis(2'-ethylhexyloxy)benzene (1a). A solution of KOH (35.07 g, 0.63 mol) in 50 mL of ethanol was slowly added to a stirred solution of catechol (27.53 g, 0.25 mol) in 150 mL of ethanol. The reaction mixture was stirred at room temperature for 1 h. A solution of 2-ethylhexyl bromide (119.87 g, 0.75 mol) in 50 mL of ethanol was added dropwise. The reaction mixture was refluxed overnight. Ethanol was removed by rotary evaporation and the reaction mixture was partitioned between ethyl acetate and sodium carbonate solution. After drying over sodium sulfate, the product was obtained by column chromatography using hexane as the eluent. A colorless oil (44.30 g) was obtained in 53% yield. MS: m/z 334. FT-IR (cm^{-1}): 3064, 3037, 2959, 2929, 2873, 2860, 1592, 1506, 1465, 1254, 1222, 1123, 1032, 737. ^1H NMR (ppm) (300 MHz, CDCl_3): δ 6.88 (s, 4H), 3.86–3.84 (d, $J = 5.62$ Hz, 4H), 1.79–1.71 (m, $J = 6.02$ Hz, 2H), 1.54–1.23 (m, 16H), 0.95–0.83 (m, 12H). ^{13}C NMR (ppm) (75.5 MHz, CDCl_3): δ 149.54, 120.76, 113.77, 71.51, 39.53, 30.55, 29.08, 23.85, 23.04, 14.04, 11.11. Anal. Calcd for $\text{C}_{22}\text{H}_{38}\text{O}_2$: C, 79.04; H, 11.38. Found: C, 78.56; H, 11.58.

Synthesis of 4,5-bis(2'-ethylhexyloxy)-1,2-dibromobenzene (1b). A solution of bromine (17.20 g, 0.11 mol) in 200 mL of glacial acetic acid was added to a solution of 1,2-bis(2'-ethylhexyloxy)benzene (1a) (18.00 g, 50 mmol) in 600 mL of a mixture of methanol and chloroform at 0 °C. The reaction mixture was stirred for 2 h, after which it was basified by addition to sodium carbonate (10%, 1000 mL) and extracted with dichloromethane (2×500 mL). The combined organic layers were washed with water (200 mL) and dried over anhydrous sodium sulfate. Column chromatography using hexane as the eluent yielded a colorless oil (24.60 g) in 93% yield. MS: m/z 492. FT-IR (cm^{-1}): 3083, 2959, 2928, 2872, 2859, 1497, 1464, 1381, 1351, 1249, 1202, 1029, 846, 652. ^1H NMR (ppm) (300 MHz, CDCl_3): δ 7.05 (s, 2H), 3.82–3.80 (d, $J = 5.62$ Hz, 4H), 1.75–1.69 (m, $J = 5.89$ Hz, 2H), 1.53–1.28 (m, 16H), 0.94–0.83 (m, 12H). ^{13}C NMR (ppm) (75.5 MHz, CDCl_3): δ 149.30, 117.60, 114.33, 71.79, 39.34, 30.40, 28.96, 23.79, 22.91, 13.94, 11.02. Anal. Calcd for $\text{C}_{22}\text{H}_{36}\text{Br}_2\text{O}_2$: C, 53.66; H, 7.32; Br, 32.52. Found: C, 53.66; H, 7.17; Br, 31.26.

Synthesis of Phenylboronic Acid (1bi). To a suspension of magnesium turnings (5.76 g, 0.24 mol) in anhydrous THF was added a solution of bromobenzene (31.40 g, 0.20 mol) in anhydrous THF. After refluxing for 4 h, the mixture was cooled to -78 °C and transferred dropwise into a solution of trimethyl borate (113.5 mL, 1 mol) in anhydrous THF. The reaction mixture was stirred at room temperature for 24 h, followed by the addition of 500 mL of 2 M HCl and stirring for 24 h. The reaction mixture was then partitioned between ether and water. Recrystallization from acetone gave white crystals (12.91 g) in 53% yield. Mp: 217.5–218.5 °C (lit. mp: 216 °C).²⁸ FT-IR (cm^{-1}): 3273, 3077, 3051, 3026, 1965, 1915, 1829, 1780, 1699, 1604, 1573, 1560, 1496, 1444, 1395, 1181, 1088, 1023,

927, 760, 698, 637, 576. ^1H NMR (ppm) (300 MHz, acetone- d_6): δ 7.88–7.85 (m, 2H), 7.41–7.31 (m, 3H), 7.10 (s, 2H). ^{13}C NMR (ppm) (75.5 MHz, acetone- d_6): δ 135.62, 133.94, 131.72, 128.97. Anal. Calcd for $\text{C}_6\text{H}_7\text{BO}_2$: C, 59.10; H, 5.79. Found: C, 58.86; H, 5.53.

Synthesis of 4,5-Bis(2'-ethylhexyloxy)-1-bromo-2-phenylbenzene (1bi). Under nitrogen atmosphere, phenylboronic acid (1bi) (1.22 g, 10 mmol), 4,5-bis(2'-ethylhexyloxy)-1,2-dibromobenzene (1b) (4.48 g, 9.1 mmol), 200 mL of THF, 200 mL of 2 M Na_2CO_3 , and tetrakis(triphenylphosphine)palladium were refluxed at 70 °C for 12 h. Partitioning between dichloromethane and water, followed by column chromatography using hexane as the eluent, gave a colorless oil (1.05 g) in 24% yield. MS: m/z 488, 490 (53%, 54%). FT-IR (cm^{-1}): 3058, 3028, 2958, 2928, 2869, 1599, 1560, 1511, 1485, 1466, 1381, 1329, 1307, 1253, 1233, 1197, 1029, 909, 857, 764, 734, 701, 647. ^1H NMR (ppm) (300 MHz, CDCl_3): δ 7.44–7.34 (m, 5H), 7.15 (s, 1H), 6.87 (s, 1H), 3.92–3.91 (d, $J = 5.64$ Hz, 2H), 3.88–3.86 (d, $J = 5.61$ Hz, 2H), 1.83–1.76 (m, $J = 5.62$ Hz, 2H), 1.61–1.31 (m, 16H), 1.01–0.90 (m, 12H). ^{13}C NMR (ppm) (75.5 MHz, CDCl_3): δ 149.29, 148.64, 141.23, 134.52, 129.48, 127.83, 127.17, 117.51, 115.99, 112.23, 71.78, 71.72, 39.49, 39.46, 30.51, 29.03, 23.86, 23.00, 13.98, 11.11, 11.08. Anal. Calcd for $\text{C}_{28}\text{H}_{41}\text{BrO}_2$: C, 68.71; H, 8.38; Br, 16.36. Found: C, 68.46; H, 8.15; Br, 16.50.

Synthesis of *p*-Xyleneboronic Acid (1ci). 1ci was synthesized according to the procedure described for 1bi using magnesium turnings (5.76 g, 0.24 mol), 2-bromo-*p*-xylene (37.00 g, 0.20 mol) and trimethyl borate (113.5 mL, 1.0 mol) to give white crystals (19.27 g) in 64% yield. Mp: 191.1–192.5 °C. FT-IR (cm^{-1}): 3293, 3104, 3014, 2968, 2921, 2862, 1906, 1860, 1809, 1767, 1609, 1573, 1493, 1418, 1064, 815, 745, 712, 686, 607, 507. ^1H NMR (ppm) (300 MHz, acetone- d_6): δ 7.38 (br s, 1H), 7.06–7.01 (m, 2H), 6.98 (s, 2H), 2.43 (s, 3H), 2.25 (s, 3H). ^{13}C NMR (ppm) (75.5 MHz, acetone- d_6): δ 140.52, 135.99, 135.93, 131.32, 131.29, 130.95, 22.81, 21.66. Anal. Calcd for $\text{C}_8\text{H}_{11}\text{BO}_2$: C, 64.07; H, 7.39. Found: C, 63.46; H, 7.15.

Synthesis of 2-(4',5'-Bis(2''-ethylhexyloxy)-2'-phenyl)-phenyl-*p*-xylene (1d). 1d was synthesized according to the procedure described for 1c using *p*-xyleneboronic acid (1ci) (0.96 g, 6 mmol) and 4,5-bis(2'-ethylhexyloxy)-1-bromo-2-phenylbenzene (1c) (1.05 g, 2 mmol) to give a colorless oil (0.95 g) in 86% yield. MS: m/z 514. FT-IR (cm^{-1}): 3027, 2958, 2927, 2867, 1602, 1515, 1490, 1465, 1380, 1346, 1243, 1194, 1164, 1133, 1035, 866, 810, 772, 699. ^1H NMR (ppm) (300 MHz, CDCl_3): δ 7.16–7.08 (m, 5H), 6.99 (br s, 1H), 6.95 (s, 1H), 6.94–6.93 (m, 2H), 6.78 (s, 1H), 3.95–3.93 (d, $J = 5.61$ Hz, 2H), 3.89–3.88 (d, $J = 5.61$ Hz, 2H), 2.28 (s, 3H), 1.83 (s, 3H), 1.83–1.76 (m, 2H), 1.58–1.27 (m, 16H), 0.99–0.89 (m, 12H). ^{13}C NMR (ppm) (75.5 MHz, CDCl_3): δ 148.44, 148.24, 141.55, 141.13, 134.42, 133.25, 132.92, 132.67, 131.38, 129.48, 129.25, 127.50, 127.44, 125.88, 115.84, 115.14, 71.71, 71.68, 39.63, 39.56, 30.56, 29.06, 23.89, 23.86, 23.00, 20.83, 20.79, 19.46, 19.43, 13.98, 11.15, 11.12. Anal. Calcd for $\text{C}_{36}\text{H}_{50}\text{O}_2$: C, 84.05; H, 9.73. Found: C, 83.67; H, 9.27.

Synthesis of 1,4-Bis(hydroxymethyl)-2-(2'-phenyl-4',5'-bis(2''-ethylhexyloxy) phenyl)benzene (1e). A mixture of 2-(4',5'-bis(2''-ethylhexyloxy)-2'-phenyl)-*p*-xylene (0.95 g, 2 mmol) (1d), *N*-bromosuccinimide (0.72 g, 4 mmol) and 2,2'-azobis(2-methylpropionitrile) (AIBN) (20 mg) in benzene (5 mL) was heated at reflux for 6 h. After cooling, the solvent was removed and the mixture was partitioned between ethyl acetate and water. The organic layer was dried over Na_2SO_4 , and the solvent was removed to give a brown oil (1.48 g) containing a mixture of brominated products. A mixture of the crude residue and anhydrous potassium acetate (4 g) in glacial acetic acid (8 mL) was heated at reflux for 16 h. After cooling, the mixture was partitioned between dichloromethane and water. The organic layer was dried over Na_2SO_4 and the solvent was removed to give a brown oil (1.11 g) containing a mixture of acetylated products. A mixture of the crude residue was added dropwise to a suspension of LiAlH_4 (0.35 g) in 5 mL of THF and stirred at room temperature overnight. Saturated Na_2SO_4 was added carefully, the reaction mixture

was filtered and dried over Na_2SO_4 , and the solvent was removed to give a brown oil. The residue was chromatographed on silica gel using hexane:ethyl acetate (10:1) as the eluent to yield colorless crystals (0.70 g) in 70% yield. Mp: 111.4–112.6 °C. MS: m/z 546. FT-IR (cm^{-1}): 3382, 3309, 3052, 3026, 2958, 2925, 2869, 1518, 1492, 1465, 1416, 1243, 1195, 1024, 822, 702. ^1H NMR (ppm) (300 MHz, CDCl_3): δ 7.35–7.33 (d, $J = 8.04$ Hz, 1H), 7.29–7.25 (dd, $J = 8.04, 1.59$ Hz, 1H), 7.23 (br s, 1H), 7.20–7.08 (m, 5H), 6.97 (s, 1H), 6.83 (s, 1H), 4.67 (s, 2H), 4.31–4.27 (d, $J = 13.23$ Hz, 1H), 4.16–4.12 (d, $J = 12.84$ Hz, 1H), 3.96–3.94 (d, $J = 5.22$ Hz, 2H), 3.90–3.88 (d, $J = 5.61$ Hz, 2H), 1.82–1.74 (m, $J = 6.02$ Hz, 2H), 1.63–1.35 (m, 16H), 0.99–0.91 (m, 12H). ^{13}C NMR (ppm) (75.5 MHz, CDCl_3): δ 148.95, 148.58, 141.00, 140.26, 139.71, 138.05, 133.04, 130.90, 129.56, 129.48, 128.23, 127.84, 126.31, 125.86, 115.84, 115.07, 71.76, 71.71, 64.94, 62.69, 39.61, 39.58, 30.54, 29.08, 29.02, 23.91, 23.86, 22.97, 13.96, 11.10. Anal. Calcd for $\text{C}_{36}\text{H}_{50}\text{O}_4$: C, 79.12; H, 9.16. Found: C, 79.30; H, 9.19.

Synthesis of 1,4-Bis(chloromethyl)-2-(2'-phenyl-4',5'-bis(2''-ethylhexyloxy) phenyl)benzene (1f). A mixture of 1,4-bis(hydroxymethyl)-2-(2'-phenyl-4',5'-bis(2''-ethylhexyloxy)-phenyl)benzene (**1e**) (0.70 g, 1.3 mmol) and thionyl chloride (1.4 mL, 19 mmol) was refluxed at 79 °C overnight. On completion of the reaction, the mixture poured into ice-cold water and partitioned between ethyl acetate and water. The organic layer was dried over Na_2SO_4 and the solvent was removed to give a brown oil. The residue was chromatographed on silica gel using hexane:ethyl acetate (100:1) as the eluent to yield a colorless oil (0.56 g) in 75% yield. MS: m/z 582, 584 (12%, 8%). FT-IR (cm^{-1}): 3057, 3014, 2958, 2927, 2873, 1601, 1518, 1464, 1383, 1249, 1199, 1033, 868, 781, 703. ^1H NMR (ppm) (300 MHz, CDCl_3): δ 7.42–7.40 (d, $J = 8.04$ Hz, 1H), 7.30–7.27 (dd, $J = 8.01, 2.01$ Hz, 1H), 7.21–7.14 (m, 4H), 7.09–7.06 (m, 2H), 7.00 (s, 1H), 6.95 (s, 1H), 4.53–4.49 (d, $J = 11.64$ Hz, 1H), 4.48–4.44 (d, $J = 11.25$ Hz, 1H), 4.41–4.37 (d, $J = 11.64$ Hz, 1H), 4.26–4.22 (d, $J = 11.64$ Hz, 1H), 3.99–3.95 (overlapping d, 4H), 1.84–1.79 (m, $J = 5.35$ Hz, 2H), 1.65–1.31 (m, 16H), 1.03–0.87 (m, 12H). ^{13}C NMR (ppm) (75.5 MHz, CDCl_3): δ 149.16, 148.46, 141.43, 140.75, 136.98, 135.64, 133.53, 131.59, 130.13, 129.76, 129.46, 127.79, 127.42, 126.26, 115.74, 115.20, 71.67, 63.65, 45.48, 43.77, 39.65, 39.58, 34.59, 34.44, 31.50, 30.61, 29.11, 26.84, 25.21, 23.94, 23.00, 22.56, 13.98, 11.15. Anal. Calcd for $\text{C}_{36}\text{H}_{48}\text{Cl}_2\text{O}_2$: C, 74.10; H, 8.23; Cl, 12.18. Found: C, 73.35; H, 8.25; Cl, 11.63.

Synthesis of Poly[2-(2'-phenyl-4',5'-bis(2''-ethylhexyloxy)phenyl)-1,4-phenylenevinylene] (BEH2P-PPV). A solution of 1,4-bis(chloromethyl)-2-(2'-phenyl-4',5'-bis(2''-ethylhexyloxy) phenyl)benzene (**1f**) (0.32 g, 0.55 mmol) in 7 mL of anhydrous THF was added to a solution of 1 M potassium *tert*-butoxide (3.3 mL) in 14 mL of anhydrous THF at room temperature with stirring for 20 h. The mixture was poured into methanol, and the resulting yellow precipitate was collected by filtration and reprecipitated from methanol. Soxhlet extraction using methanol followed by acetone gave a bright yellow polymer (220 mg) in 79% yield. FT-IR (cm^{-1}): 3052, 3026, 2956, 2925, 2864, 1600, 1514, 1488, 1465, 1380, 1344, 1239, 1178, 1031, 963, 863, 768, 698. ^1H NMR (ppm) (300 MHz, CDCl_3): δ 7.46, 7.36, 7.04, 6.85, 6.67 (aromatic, 12H), 3.92 (4H), 1.78 (2H), 1.49–1.33 (16H), 0.91 (12H). Anal. Calcd for $\text{C}_{36}\text{H}_{46}\text{O}_2$: C, 84.71; H, 9.02. Found: C, 82.92; H, 8.85.

Synthesis of 1,3-Bis(2'-ethylhexyloxy)benzene (2a). **2a** was synthesized according to the procedure described for **1a** using KOH (35.0 g, 0.63 mol), resorcinol (27.5 g, 0.25 mol), and 2-ethylhexyl bromide (119.9 g, 0.75 mol) to give a colorless oil (43.95 g) in 53% yield. MS: m/z 334. FT-IR (cm^{-1}): 3064, 3037, 2959, 2929, 2873, 2860, 1592, 1506, 1465, 1254, 1222, 1123, 1032, 737. ^1H NMR (ppm) (300 MHz, CDCl_3): δ 6.88 (s, 4H), 3.86–3.84 (d, $J = 5.62$ Hz, 4H), 1.79–1.71 (m, $J = 6.02$ Hz, 2H), 1.54–1.23 (m, 16H), 0.95–0.83 (m, 12H). ^{13}C NMR (ppm) (75.5 MHz, CDCl_3): δ 160.58, 129.56, 106.48, 101.41, 70.36, 39.33, 30.48, 29.01, 23.81, 22.97, 13.98, 11.01. Anal. Calcd for $\text{C}_{22}\text{H}_{38}\text{O}_2$: C, 79.04; H, 11.38. Found: C, 79.10; H, 11.34.

Synthesis of 1,5-Bis(2'-ethylhexyloxy)-2,4-dibromobenzene (2b). **2b** was synthesized according to the procedure described for **1b** using bromine (17.20 g, 0.11 mol) and 1,3-bis(2'-ethylhexyloxy)benzene (**2a**) (18.00 g, 50 mmol) to give a colorless oil (24.62 g) in 93% yield. MS: m/z 492. FT-IR (cm^{-1}): 3074, 2959, 2929, 2873, 2860, 1715, 1580, 1570, 1488, 1458, 1402, 1369, 1287, 1196, 1061, 924, 875, 808, 772, 728, 704, 681. ^1H NMR (ppm) (300 MHz, CDCl_3): δ 7.63 (s, 1H), 6.45 (s, 1H), 3.89–3.88 (d, $J = 5.22$ Hz, 4H), 1.81–1.73 (m, $J = 5.92$ Hz, 2H), 1.58–1.26 (m, 16H), 0.97–0.85 (m, 12H). ^{13}C NMR (ppm) (75.5 MHz, CDCl_3): δ 155.69, 135.23, 102.70, 99.26, 71.74, 39.31, 30.39, 28.99, 23.80, 22.89, 13.95, 11.09. Anal. Calcd for $\text{C}_{22}\text{H}_{36}\text{Br}_2\text{O}_2$: C, 53.66; H, 7.32; Br, 32.52. Found: C, 54.30; H, 6.91; Br, 31.68.

Synthesis of 1,5-Bis(2'-ethylhexyloxy)-4-bromo-2-phenylbenzene (2c). **2c** was synthesized according to the procedure described for **1c** using phenylboronic acid (1.22 g, 10 mmol) and 1,5-bis(2'-ethylhexyloxy)-2,4-dibromobenzene (**2b**) (4.48 g, 9.1 mmol) to give a colorless oil (1.88 g) in 42% yield. MS: m/z 488, 490 (44%, 45%). FT-IR (cm^{-1}): 3058, 3027, 2958, 2927, 2872, 2859, 1598, 1509, 1463, 1402, 1377, 1306, 1239, 1189, 1041, 698. ^1H NMR (ppm) (300 MHz, CDCl_3): δ 7.48–7.46 (d, $J = 7.23$ Hz, 3H), 7.39–7.34 (m, $J = 7.26$ Hz, 2H), 7.30–7.26 (m, $J = 6.81$ Hz, 1H), 6.55 (s, 1H), 3.97–3.95 (d, $J = 5.22$ Hz, 2H), 3.84–3.82 (d, $J = 5.22$ Hz, 2H), 1.84–1.78 (m, $J = 5.89$ Hz, 1H), 1.66–1.25 (m, 17H), 1.01–0.83 (m, 12H). ^{13}C NMR (ppm) (75.5 MHz, CDCl_3): δ 156.33, 155.52, 134.06, 129.37, 127.71, 126.55, 124.60, 98.84, 71.51, 71.03, 39.37, 39.33, 30.43, 29.05, 28.90, 23.82, 23.79, 22.97, 22.91, 14.03, 13.96, 11.15, 11.02. Anal. Calcd for $\text{C}_{28}\text{H}_{41}\text{BrO}_2$: C, 68.71; H, 8.38; Br, 16.36. Found: C, 69.47; H, 8.10; Br, 15.41.

Synthesis of 2-(2',4'-Bis(2''-ethylhexyloxy)-5'-phenyl)-phenyl-*p*-xylene (2d). **2d** was synthesized according to the procedure described for **1c** using *p*-xyleneboronic acid (0.74 g, 5.0 mmol) and 1,5-bis(2'-ethylhexyloxy)-4-bromo-2-phenylbenzene (**2c**) (1.86 g, 3.8 mmol) to give a colorless oil (1.17 g) in 60% yield. MS: m/z 514. FT-IR (cm^{-1}): 3029, 2958, 2927, 2872, 2859, 1610, 1580, 1569, 1515, 1487, 1464, 1447, 1405, 1378, 1314, 1286, 1239, 1186, 1164, 1133, 1040, 903, 809, 770, 698. ^1H NMR (ppm) (300 MHz, CDCl_3): δ 7.58–7.54 (dd, 2H), 7.38–7.33 (m, 2H), 7.28–7.23 (m, 1H), 7.17 (s, 1H), 7.13–7.10 (m, 1H), 7.04–7.02 (m, 2H), 6.62 (s, 1H), 3.92–3.90 (d, $J = 5.22$ Hz, 2H), 3.84–3.82 (d, $J = 5.22$ Hz, 2H), 2.32 (s, 3H), 2.16 (s, 3H), 1.71–1.65 (m, 1H), 1.59–1.20 (m, 17H), 0.99–0.79 (m, 12H). ^{13}C NMR (ppm) (75.5 MHz, CDCl_3): δ 156.52, 156.18, 138.38, 138.18, 134.22, 133.76, 132.66, 131.15, 129.50, 129.18, 127.58, 127.42, 126.05, 123.95, 122.83, 98.16, 98.09, 71.05, 70.82, 39.53, 39.40, 30.58, 30.43, 28.99, 28.90, 23.92, 23.78, 22.91, 20.80, 20.76, 19.65, 19.62, 13.94, 11.10, 10.99. Anal. Calcd for $\text{C}_{36}\text{H}_{50}\text{O}_2$: C, 84.05; H, 9.73. Found: C, 83.40; H, 9.86.

Synthesis of 1,4-Bis(hydroxymethyl)-2-(2',4'-bis(2''-ethylhexyloxy)-5'-phenyl)phenylbenzene (2e). **2e** was synthesized according to the procedure described for **1e** using 2-(2',4'-bis(2''-ethylhexyloxy)-5'-phenyl)-*p*-xylene (**2d**) (1.17 g, 2 mmol), *N*-bromosuccinimide (0.89 g, 5 mmol), and 2,2'-azobis(2-methylpropionitrile) (AIBN) (20 mg) to yield colorless crystals (0.62 g) in 50% yield. Mp: 60.6–62.1 °C. MS: m/z 546. FT-IR (cm^{-1}): 3346, 3053, 3027, 2957, 2928, 1608, 1569, 1509, 1486, 1464, 1402, 1380, 1313, 1282, 1236, 1185, 1162, 1124, 1037, 902, 825, 769, 699. ^1H NMR (ppm) (300 MHz, CDCl_3): δ 7.51–7.45 (m, 3H), 7.34–7.29 (m, 3H), 7.25–7.22 (m, 1H), 7.18 (s, 1H), 7.15 (s, 1H), 6.62 (s, 1H), 4.64 (s, 2H), 4.46–4.44 (d, $J = 5.61$ Hz, 2H), 3.89–3.87 (d, $J = 5.22$ Hz, 2H), 3.72 (br s, 2H), 1.71–1.63 (m, 1H), 1.60–1.12 (m, 17H), 0.97–0.72 (m, 12H). ^{13}C NMR (ppm) (75.5 MHz, CDCl_3): δ 156.71, 156.30, 140.06, 138.99, 137.95, 137.64, 132.65, 129.47, 129.09, 128.65, 127.65, 126.34, 126.00, 123.91, 122.68, 98.95, 98.89, 72.19, 70.89, 64.91, 63.61, 39.48, 39.35, 30.56, 30.30, 28.98, 28.82, 23.91, 23.68, 22.94, 22.84, 22.58, 13.93, 11.08, 10.89. Anal. Calcd for $\text{C}_{36}\text{H}_{50}\text{O}_4$: C, 79.12; H, 9.16. Found: C, 78.69; H, 9.53.

Synthesis of 1,4-Bis(chloromethyl)-2-(2',4'-bis(2''-ethylhexyloxy)-5'-phenyl)phenylbenzene (2f). **2f** was synthesized according to the procedure as for **1f** using 1,4-

bis(hydroxymethyl)-2-(2',4'-bis(2''-ethylhexyloxy)-5'-phenyl)benzene (**2e**) (0.52 g, 0.94 mmol) and thionyl chloride (1.0 mL, 14 mmol) to yield a colorless oil (0.45 g) in 63% yield. MS: *m/z* 582, 584 (100%, 50%). FT-IR (cm⁻¹): 3027, 2958, 2928, 2868, 1608, 1579, 1510, 1463, 1401, 1379, 1315, 1262, 1239, 1188, 1168, 1116, 1043, 903, 818, 768, 699. ¹H NMR (ppm) (300 MHz, CDCl₃): δ 7.58–7.54 (m, 3H), 7.40–7.34 (m, 3H), 7.30–7.24 (m, 3H), 6.62 (s, 1H), 4.59 (s, 2H), 4.55 (s, 1H), 4.52 (s, 1H), 3.93–3.91 (d, *J* = 5.22 Hz, 2H), 3.87–3.83 (d, *J* = 13.65 Hz, 2H), 1.73–1.69 (m, *J* = 5.82 Hz, 1H), 1.57–1.54 (m, *J* = 4.82 Hz, 2H), 1.48–1.12 (m, 15H), 1.00–0.74 (m, 12H). ¹³C NMR (ppm) (75.5 MHz, CDCl₃): δ 156.95, 156.28, 138.48, 137.96, 136.89, 136.46, 132.69, 131.19, 129.58, 129.50, 127.65, 127.51, 126.25, 123.11, 120.82, 97.74, 97.67, 70.93, 70.82, 45.70, 44.27, 39.46, 39.29, 30.55, 30.43, 28.98, 28.90, 28.86, 23.89, 23.79, 22.92, 22.85, 13.93, 11.07, 10.98. Anal. Calcd for C₃₆H₄₈Cl₂O₂: C, 74.10; H, 8.23, Cl, 12.18. Found: C, 74.47; H, 7.90, Cl, 11.91.

Synthesis of Poly[2-(2',4'-bis(2''-ethylhexyloxy)-5'-phenyl)phenyl]-1,4-phenylenevinylene] (BEH3P-PPV). BEH3P-PPV was synthesized according to the procedure described for BEH2P-PPV using 1,4-bis(chloromethyl)-2-(2'-phenyl-3',5'-bis(2''-ethylhexyloxy)phenyl)benzene (**2f**) (0.35 g, 0.60 mmol) in 8 mL of anhydrous THF and 1 M potassium *tert*-butoxide (3.6 mL) in 16 mL of anhydrous THF. An orange polymer (125 mg) was obtained in 41% yield. FT-IR (cm⁻¹): 3021, 2956, 2924, 2862, 1604, 1461, 1377, 1309, 1232, 1171, 1115, 1041, 960, 898, 817, 766, 697. ¹H NMR (ppm) (300 MHz, CDCl₃): δ 7.68, 7.67, 7.50, 7.23, 7.08, 6.61 (aromatic, 12H), 3.91–3.82 (2H), 3.53 (2H), 1.68 (1H), 1.43–1.09 (17H), 0.99–0.71 (12H). Anal. Calcd for C₃₆H₄₆O₂: C, 84.71; H, 9.02. Found: C, 82.21; H, 8.31.

Synthesis of 1,4-Bis(2'-ethylhexyloxy)benzene (3a). **3a** was synthesized according to the procedure described for **1a** using KOH (35.00 g, 0.63 mol), hydroquinone (27.50 g, 0.25 mol), and 2-ethylhexyl bromide (145 g, 0.75 mol) to give a colorless oil (57.60 g) in 69% yield. MS: *m/z* 334. FT-IR (cm⁻¹): 3047, 2960, 2930, 2874, 2860, 1508, 1467, 1380, 1228, 1040, 823, 786. ¹H NMR (ppm) (300 MHz, CDCl₃): δ 6.83 (s, 4H), 3.80–3.78 (d, *J* = 6.02 Hz, 4H), 1.75–1.67 (m, *J* = 6.02 Hz, 2H), 1.58–1.29 (m, 16H), 0.96–0.72 (m, 12H). ¹³C NMR (ppm) (75.5 MHz, CDCl₃): δ 153.37, 115.29, 71.12, 39.38, 30.45, 29.01, 23.76, 22.97, 14.00, 11.01. Anal. Calcd for C₂₂H₃₈O₂: C, 79.04; H, 11.38. Found: C, 78.50; H, 11.77.

Synthesis of 2,5-Bis(2'-ethylhexyloxy)-1,4-dibromobenzene (3b). **3b** was synthesized according to the procedure described for **1b** using bromine (19.20 g, 0.12 mol) and 1,4-bis(2'-ethylhexyloxy)benzene (**3a**) (20.00 g, 60 mmol) to give a colorless oil (25.00 g) in 85% yield. MS: *m/z* 492. FT-IR (cm⁻¹): 2959, 2928, 2872, 2859, 1494, 1460, 1362, 1212, 1064, 1028, 1007, 850, 807. ¹H NMR (ppm) (300 MHz, CDCl₃): δ 7.08 (s, 2H), 3.84–3.82 (d, *J* = 5.62 Hz, 4H), 1.76–1.70 (m, *J* = 6.02 Hz, 2H), 1.57–1.26 (m, 16H), 0.96–0.83 (m, 12H). ¹³C NMR (ppm) (75.5 MHz, CDCl₃): δ 150.10, 118.12, 110.98, 72.46, 39.34, 30.35, 28.93, 23.78, 22.91, 13.94, 11.04. Anal. Calcd for C₂₂H₃₆Br₂O₂: C, 53.66; H, 7.32; Br, 32.52. Found: C, 53.96; H, 7.57; Br, 31.45.

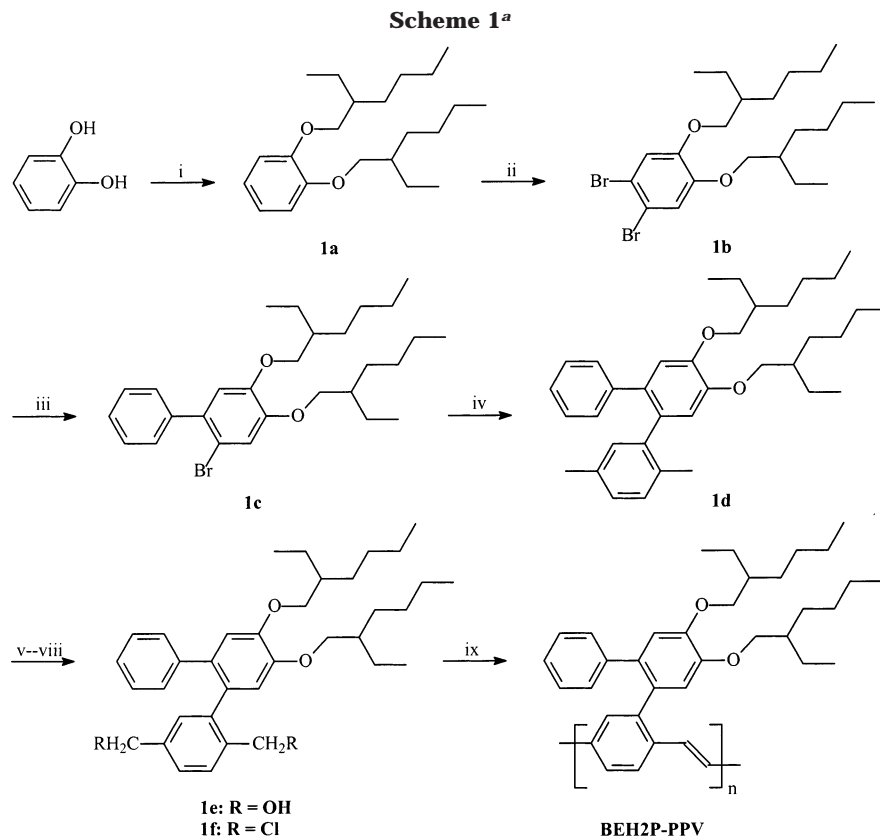
Synthesis of 2,5-Bis(2'-ethylhexyloxy)-1-bromo-4-phenylbenzene (3c). **3c** was synthesized according to the procedure described for **1c** using phenylboronic acid (0.12 g, 1 mmol) and 2,5-bis(2'-ethylhexyloxy)-1,4-dibromobenzene (**3b**) (0.50 g, 1 mmol) to give a colorless oil (0.25 g) in 51% yield. MS: *m/z* 488, 490 (23%, 24%). FT-IR (cm⁻¹): 3058, 3028, 2959, 2928, 2872, 2859, 1485, 1465, 1378, 1270, 1209, 1059, 1033, 764, 698. ¹H NMR (ppm) (300 MHz, CDCl₃): δ 7.53–7.51 (dd, *J* = 8.24, 1.40 Hz, 2H), 7.43–7.31 (m, 3H), 7.18 (s, 1H), 6.91 (s, 1H), 3.91–3.89 (d, *J* = 5.61 Hz, 2H), 3.78–3.76 (d, *J* = 5.61 Hz, 2H), 1.82–1.74 (m, *J* = 6.02 Hz, 2H), 1.63–1.24 (m, 16H), 0.99–0.82 (m, 12H). ¹³C NMR (ppm) (75.5 MHz, CDCl₃): δ 150.45, 149.90, 137.87, 130.99, 129.34, 127.76, 126.99, 118.08, 116.04, 111.10, 72.42, 71.80, 39.46, 39.36, 30.41, 28.99, 28.85, 23.82, 23.76, 22.95, 22.88, 13.97, 13.91, 12.12, 11.08, 10.95. Anal. Calcd for C₂₈H₄₁BrO₂: C, 68.71; H, 8.38; Br, 16.36. Found: C, 68.26; H, 8.88; Br, 15.98.

Synthesis of 2-(2',5'-Bis(2''-ethylhexyloxy)-4'-phenyl)phenyl-*p*-xylene (3d). A Grignard reagent of 2-bromo-mag-

nesio-*p*-xylene, prepared from the reaction of 2-bromo-*p*-xylene (1.80 g, 10 mmol) with magnesium (0.28 g, 12 mmol) in 10 mL of THF, was added dropwise into a solution of 2,5-bis(2'-ethylhexyloxy)-1-bromo-4-phenylbenzene (**3c**) (1.58 g, 3 mmol) in 20 mL of THF containing Ni(dppp)₂Cl₂ (18 mg, 0.03 mmol) as a catalyst. After refluxing overnight, the reaction mixture was quenched with 0.2 M HCl and extracted with ethyl acetate. The extract was washed with water and brine, followed by drying over anhydrous sodium sulfate. The reaction mixture was subjected to column chromatography using hexane as the eluent. A light yellow oil (1.17 g) was obtained in 40% yield. MS: *m/z* 514. FT-IR (cm⁻¹): 3056, 3032, 2959, 2927, 2872, 1508, 1487, 1408, 1379, 1205, 1057, 872, 808, 767, 698. ¹H NMR (ppm) (300 MHz, CDCl₃): δ 7.63–7.59 (m, 2H), 7.44–7.37 (m, 2H), 7.32–7.31 (m, 1H), 7.15–7.13 (m, 1H), 7.07–7.05 (m, 2H), 6.96 (s, 1H), 6.81 (s, 1H), 3.76–3.74 (d, *J* = 5.61 Hz, 2H), 3.73–3.71 (d, *J* = 5.22 Hz, 2H), 2.35 (s, 3H), 2.18 (s, 3H), 1.80–1.16 (m, 18H), 0.96–0.73 (m, 12H). ¹³C NMR (ppm) (75.5 MHz, CDCl₃): δ 149.82, 149.74, 138.41, 138.35, 134.34, 133.53, 130.91, 130.80, 130.02, 129.55, 129.33, 128.21, 127.64, 127.59, 127.42, 126.47, 115.92, 115.54, 71.75, 71.72, 39.48, 39.40, 30.47, 30.41, 29.03, 28.92, 23.85, 23.81, 22.86, 20.82, 20.78, 19.54, 14.05, 13.95, 11.06, 10.98. Anal. Calcd for C₃₆H₅₀O₂: C, 84.05; H, 9.73. Found: C, 83.93; H, 9.84.

Synthesis of 1,4-Bis(hydroxymethyl)-2-(2',5'-bis(2''-ethylhexyloxy)-4'-phenyl)phenylbenzene (3e). A mixture of 2-(2',5'-bis(2''-ethylhexyloxy)-4'-phenyl)-*p*-xylene (**3d**) (1.17 g, 2 mmol), *N*-bromosuccinimide (0.89 g, 5 mmol) and 2,2'-azobis(2-methylpropionitrile) (20 mg) in benzene (2 mL) was heated at reflux for 6 h. After cooling, the solvent was removed, and the mixture was partitioned between ethyl acetate and water. The organic layer was dried over Na₂SO₄, and the solvent was removed to give a brown oil (2.33 g) containing a mixture of brominated products. A mixture of the crude residue and anhydrous potassium acetate (4 g) in glacial acetic acid (8 mL) was heated at reflux for 16 h. After cooling, the mixture was partitioned between dichloromethane and water. The organic layer was dried over Na₂SO₄, and the solvent was removed to give a brown oil (3.20 g) containing a mixture of acetylated products. A mixture of the crude residue, methanol (15 mL), and 10% sodium hydroxide (15 mL) was heated at reflux for 2 h. After cooling, the mixture was partitioned between dichloromethane and water. The organic layer was dried over Na₂SO₄ and the solvent was removed to give a brown oil. The residue was chromatographed on silica gel using hexane:ethyl acetate (10:1) as the eluent to yield a pale yellow oil (0.48 g) in 40% yield. MS: *m/z* 546. FT-IR (cm⁻¹): 3403, 3056, 3027, 2958, 2928, 2871, 1513, 1486, 1463, 1419, 1379, 1205, 1032, 768, 698. ¹H NMR (ppm) (300 MHz, CDCl₃): δ 7.60–7.57 (m, 2H), 7.56–7.53 (d, *J* = 8.04 Hz, 1H), 7.44–7.28 (m, 5H), 7.01 (s, 1H), 6.82 (s, 1H), 4.74 (s, 2H), 4.53–4.49 (d, *J* = 11.64 Hz, 1H), 4.45–4.41 (d, *J* = 12.45 Hz, 1H), 3.84 (br s, OH), 3.77–3.75 (d, *J* = 5.22 Hz, 2H), 3.71–3.70 (d, *J* = 5.22 Hz, 2H), 3.60 (br s, OH), 1.63–1.53 (m, *J* = 6.02 Hz, 1H), 1.45–1.09 (m, 17H), 0.86–0.68 (m, 12H). ¹³C NMR (ppm) (75.5 MHz, CDCl₃): δ 150.76, 150.02, 140.11, 138.86, 138.09, 137.93, 131.28, 130.60, 129.48, 129.21, 128.53, 127.74, 126.89, 126.37, 117.35, 115.55, 71.58, 65.00, 62.28, 39.45, 39.39, 30.43, 30.22, 28.86, 28.79, 23.78, 23.60, 22.88, 22.82, 22.79, 13.91, 10.97. Anal. Calcd for C₃₆H₅₀O₄: C, 79.12; H, 9.16. Found: C, 79.59; H, 9.23.

Synthesis of 1,4-Bis(chloromethyl)-2-(2',5'-bis(2''-ethylhexyloxy)-4'-phenyl)phenylbenzene (3f). **3f** was synthesized according to the procedure as for **1f** using 1,4-bis(hydroxymethyl)-2-(4'-phenyl-2',5'-bis(2''-ethylhexyloxy)phenyl)benzene (**3e**) (0.39 g, 0.72 mmol) and thionyl chloride (0.8 mL, 10 mmol) to yield a colorless oil (0.31 g) in 75% yield. MS: *m/z* 582, 584 (100%, 50%). FT-IR (cm⁻¹): 3055, 3028, 2958, 2928, 2871, 1513, 1486, 1464, 1420, 1379, 1262, 1206, 1033, 768, 699. ¹H NMR (ppm) (300 MHz, CDCl₃): δ 7.63–7.57 (m, 3H), 7.46–7.32 (m, 5H), 6.98 (s, 1H), 6.95 (s, 1H), 4.63–4.60 (m, 2H), 4.57–4.55 (d, *J* = 6.84 Hz, 2H), 3.82–3.80 (d, *J* = 5.64 Hz, 2H), 3.75–3.73 (d, *J* = 5.22 Hz, 2H), 1.64–1.60 (m, 1H), 1.58–1.14 (m, 17H), 0.90–0.62 (m, 12H). ¹³C



^a Reagents and conditions: i, KOH/EtOH, 2-ethylhexyl bromide; ii, Br₂/AcOH; iii, phenylboronic acid, 2 M Na₂CO₃, Pd(PPh₃)₄; iv, 2-bromo-*p*-xylene, 2 M Na₂CO₃, Pd(PPh₃)₄; v, *N*-bromosuccinimide (NBS)/AIBN/benzene; vi, KOAc/AcOH; vii, LiAlH₄/THF; viii, SOCl₂; ix, *tert*-BuOK/THF.

NMR (ppm) (75.5 MHz, CDCl₃): δ 150.10, 150.04, 138.49, 138.29, 136.99, 136.23, 131.50, 130.85, 130.07, 129.82, 129.52, 128.32, 127.80, 127.74, 127.60, 126.87, 116.01, 115.61, 71.72, 45.64, 44.27, 39.45, 39.36, 30.45, 30.39, 28.85, 23.79, 23.73, 22.91, 22.85, 22.59, 14.01, 13.91, 10.98, 10.91. Anal. Calcd for C₃₆H₄₈Cl₂O₂: C, 74.10; H, 8.23, Cl, 12.18. Found: C, 73.28; H, 8.62, Cl, 11.25.

Synthesis of Poly[2-(2',5'-bis(2''-ethylhexyloxy)-4'-phenyl)phenyl-1,4-phenylenevinylene] (BEH4P-PPV). BEH4P-PPV was synthesized according to the procedure described for BEH2P-PPV using 1,4-bis(chloromethyl)-2-[4'-phenyl-2',5'-bis(2''-ethylhexyloxy)phenyl]benzene (**3f**) (0.17 g, 0.30 mmol) in 4 mL of anhydrous THF and 1 M potassium *tert*-butoxide (1.78 mL) in 8 mL of anhydrous THF. A bright yellow polymer (83 mg) was obtained in 55% yield. FT-IR (cm⁻¹): 3058, 3027, 2956, 2862, 1510, 1463, 1376, 1203, 1031, 961, 767, 696. ¹H NMR (ppm) (300 MHz, CDCl₃): δ 7.60, 7.38, 7.34, 6.99, 6.85 (aromatic, 12H), 3.71 (4H), 1.23–1.08 (18H), 0.80–0.72 (12H). Anal. Calcd for C₃₆H₄₆O₂: C, 84.71; H, 9.02. Found: C, 83.41; H, 8.84.

Results and Discussion

Synthesis and Characterization. The synthetic route to 2EH-PPV and 4EH-PPV is similar to the procedure described in ref 27. 2-Bromophenol or 4-bromophenol was used as a starting material for the synthesis of 1-bromo-2-(2'-ethylhexyloxy)benzene or 1-bromo-4-(2'-ethylhexyloxy)benzene through the Williamson ether synthesis. The ether products were coupled with the Grignard reagent of 2-bromo-*p*-xylene to yield 2-(2'-(2''-ethylhexyloxy)phenyl)-*p*-xylene or 2-(4'-(2''-ethylhexyloxy)phenyl)-*p*-xylene. A multistep procedure starting with NBS bromination, esterification of the brominated products, followed by reduction of the acetylated products to yield dihydroxylated compounds, and finally reaction with thionyl chloride afforded the

monomer 1,4-bis(chloromethyl)-2-(2'-(2''-ethylhexyloxy)-phenyl)benzene or 1,4-bis(chloromethyl)-2-(4'-(2''-ethylhexyloxy)phenyl)benzene. Polymerization at room temperature according to the Gilch route using *tert*-BuOK as the base and THF as the solvent afforded the light yellow (2EH-PPV) and orange polymers (4EH-PPV), respectively.

In the synthesis of BEH2P-PPV, BEH3P-PPV, and BEH4P-PPV, catechol, resorcinol, and hydroquinone were used as the starting materials, respectively. The synthetic procedure for BEH2P-PPV as an example is depicted in Scheme 1. After Williamson ether reaction, nuclear bromination of **1a** was effected using bromine in glacial acetic acid to give 4,5-bis(2'-ethylhexyloxy)-1,2-dibromobenzene (**1b**). The Suzuki coupling reaction of phenylboronic acid (**1bi**) with **1b** yielded 4,5-bis(2'-ethylhexyloxy)-1-bromo-2-phenylbenzene (**1c**) which was subsequently reacted with *p*-xyleneboronic acid or the Grignard reagent of 2-bromo-*p*-xylene to give 2-(2'-phenyl-4',5'-bis(2''-ethylhexyloxy)phenyl)-*p*-xylene (**1d**). The reason for employing the Suzuki reaction for the synthesis of **1c**, **2c**, and **3c** was because it was found that a higher yield resulted, which is probably due to the higher selectivity of the Suzuki coupling reaction as compared to that of the Grignard coupling reaction. Both Suzuki and Grignard coupling reactions can be exploited for the following synthesis of **1d**, **2d**, and **3d** with satisfactory yields. The monomer 1,4-bis(chloromethyl)-2-(2'-phenyl-4',5'-bis(2''-ethylhexyloxy)phenyl)benzene (**1f**) was obtained through a multistep procedure starting with NBS bromination of **1d**, esterification of the brominated products, followed by reduction of the acetylated products to 1,4-bis(hydroxymethyl)-2-(2'-phenyl-4',5'-bis(2''-ethylhexyloxy)phenyl)benzene (**1e**),

Table 1. Effect of Solvent Polarity on the Amount of TBB in 4EH-PPV

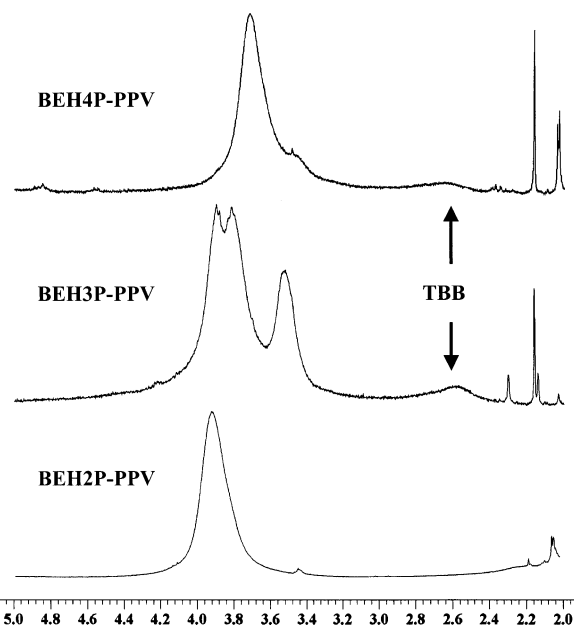
solvent	solvent polarity	amount of TBB (%)
THF	21	2.55
1,4-dioxane	16.4	3.18
<i>p</i> -xylene	7.4	4.64

and finally reaction with thionyl chloride. Polymerization at room temperature according to the Gilch route using *t*-BuOK as the base and THF as the solvent afforded the bright yellow polymer. The synthetic routes to **BEH3P-PPV** and **BEH4P-PPV** are essentially the same as that of **BEH2P-PPV**, except that the starting materials used were resorcinol and hydroquinone, respectively. **BEH3P-PPV** was obtained as an orange polymer while **BEH4P-PPV** was a bright yellow polymer. The polymers were fully soluble at room temperature in common organic solvents such as CHCl₃, THF, toluene, and *p*-xylene.

One of the main efforts of this work is to seek an effective way to suppress the structural defects in the polymers. Therefore, the amount of tolane-bisbenzyl (TBB) defects in this series of polymers was estimated by the integration of a small signal around 2.4–2.8 ppm in the proton NMR spectra, relative to that of the alkoxy protons. For **2EH-PPV** and **4EH-PPV**, 2.46% and 2.55% of TBB were observed, respectively. This is significantly lower as compared to DOP-PPV²⁷ or Ph-PPVs,^{23,25} DOP-PPV and Ph-PPVs, results of polymerization in which *o*-xylene and 1,4-dioxane were used as the solvent, possessed 5.99% and 5–6% TBB defects, respectively. Hence, we postulate that the solvent in which polymerization takes place plays a very important role in the amount of TBB defects observed.

The effect of polymerization solvent on the amount of TBB defects was thus investigated. The monomer of **4EH-PPV** was polymerized under identical conditions with the exception of the polymerization solvent used. Three different solvents, THF, 1,4-dioxane, and *p*-xylene, were used, and the amounts of TBB defects observed in the polymers were 2.55%, 3.18% and 4.64% respectively. Hence, a very obvious trend can be identified for the relationship between the polarity of the solvent and the amount of TBB observed. The relationship is an inverse one where the higher the polarity of the solvent, the lower is the amount of TBB observed. The solvent polarity quoted as follows is referenced against water, which has a value of 100.²⁹ The results are summarized in Table 1. As a solvent for the Gilch polymerization, THF would be the most ideal solvent for minimizing the amount of TBB defects observed.

From the phenomenon of solvent polarity affecting the formation of structural defects in polymers, it may be interpreted that solvents can influence the polymerization process. The mechanism of the Gilch route to prepare PPVs is still arguable. Both radical and anionic chain reactions have been proposed.^{30–33} However, a dual reaction mechanism, which involves both processes, is more reasonable.^{34,35} During chain propagation, both radical and anionic species may form head-to-head or tail-to-tail irregular linkage. However, the possibility of irregularity from the anionic reaction is lower than that from the radical reaction due to electronic effects. It is well-known that polar solvents can accelerate the anionic chain propagation due to the stronger coordination effect of polar solvents to anionic species.³⁶ On the other hand, the polarity has no significant effect on the radical reaction. Therefore, it

**Figure 2.** ¹H NMR showing the TBB signal at 2.4–2.8 ppm.

is rational to conclude that polymerization in more polar solvents such as THF will result in a low amount of head-to-head and tail-to-tail linkage due to anionic polymerization dominating the chain propagation.

Besides the effect of solvents, the monomer structure, which is associated with electronic property and steric effect of the substituents, will also influence the polymerization process. The effect of electronic property of substituents on the monomer has been demonstrated by COVION.^{23,26} The steric effect will be discussed here. From the model polymers **2EH-PPV** and **4EH-PPV**, we can find that the introduction of the alkoxy side chain at the ortho-position of the side phenyl ring (**2EH-PPV**) is not as efficient in suppressing the irregular structure formation, as compared to **4EH-PPV**. Therefore, a structure with more hindrance is required to achieve this target. In the new series of polymers, **BEH2P-PPV**, **BEH3P-PPV**, and **BEH4P-PPV**, the amount of TBB observed was found to be 0.36%, 3.79%, and 3.72%, respectively. Among the three polymers, **BEH2P-PPV** contains the lowest amount of TBB, which is in accordance with our expectation. Their ¹H NMR spectra, in which the signals of TBB can be found around 2.4–2.8 ppm, are shown in Figure 2. Because of the highly rigid structure of **BEH2P-PPV**, the phenyl substituent in position-2 of the side chain imposes great steric hindrance during the polymerization process, hence minimizing abnormal head-to-head linkages and thus dramatically reducing the amount of TBB defects observed. The effect of steric hindrance on the amount of TBB defects can be explained by the mechanism, which is illustrated in Scheme 2. When the monomer reacts with 1 mol of the base, both of the chloromethyl groups can be deprotonated. If the monomer is asymmetric, attack of either of the two chloromethyl groups gives rise to two different xylylene “real” monomers, leading to a certain amount of TBB defects. In the case of **BEH2P-PPV**, the bulky substituent on position-2 on the side group allows the base to attack only the sterically less hindered chloromethyl group. Hence, only one xylylene intermediate results and on propagation of the regular head-to-tail linkage, the formation of TBB defects is suppressed. As a result, negligible TBB defects were detected in **BEH2P-PPV**

as compared to **BEH3P-PPV** and **BEH4P-PPV**. In Scheme 2, two possible routes based on the anionic chain reaction were illustrated to explain the polymerization process. In fact, the mechanism is also applicable to the radical polymerization process.

The influence of tolane-bisbenzyl structural defects on the device performance is still under investigation. It is suggested that the tolane-bisbenzyl moieties will lower the charge carrier mobility due to an interruption of the π -conjugation along the polymer chains, which may lead to charge carrier build up, resulting in additional breaks in conjugation.^{23,37} This is a self-accelerating process of degradation. In addition, the active benzyl groups of the structural defects may also be converted to carbonyl groups through photooxidation or electro-oxidation during device operation. The newly generated exciton trapping sites will reduce the device quantum efficiency. In fact, a similar phenomenon has recently been reported in poly(dialkylfluorene)-based LED devices.³⁸ Both channels will lead to a higher driving voltage to operate the device at a constant current. Therefore, the tolane-bisbenzyl structural defects may not directly influence the efficiency of the as-prepared LED devices but more of the performance during the aging test. Since the amount of TBB defects adversely affects the device efficiency and lifetime of PLEDs, **BEH2P-PPV** would be expected to demonstrate the best performance as compared to the other polymers when used as the emissive layer in PLEDs.

Besides investigation of TBB formation in the polymers, their physical, optical, and electrochemical properties have also been studied. GPC analysis revealed that the number-average molecular weights (M_n) of the polymers **BEH2P-PPV**, **BEH3P-PPV**, and **BEH4P-PPV** were 3.6×10^5 , 1.3×10^5 , and 5.7×10^5 respectively while the weight-average molecular weights (M_w) were 7.7×10^5 , 3.1×10^5 and 9.2×10^5 with a polydispersity indexes of 2.11, 2.45, and 1.61, respectively. The onsets of degradation of the polymers **BEH2P-PPV**, **BEH3P-PPV**, and **BEH4P-PPV** were observed through thermogravimetric analysis (TGA) in nitrogen to be 314, 339, and 300 °C, respectively, indicating good thermal stability, an essential property for application of the polymers in PLEDs. No obvious T_g was observed from this series of polymers.

Optical and Photoluminescence Properties. The absorption and photoluminescence (PL) spectra of the polymer solutions in CHCl_3 and that of the polymer films spin-cast from xylene solutions were measured at room temperature. On comparison of the spectra of polymers (Figures 3 and 4), it can be seen that the polymers show structureless absorption spectra except for **BEH4P-PPV**, where an additional peak was observed at 316 nm for the solution sample and at 317 nm for the film sample. These peaks are a result of absorption due to the full conjugation of the three phenyl rings in the side chain. The UV λ_{max} of **BEH2P-PPV** is slightly blue shifted as compared to those of **BEH3P-PPV** and **BEH4P-PPV**. This should be due to the steric hindrance caused by the bulky phenyl ring in position-2 on the side group, resulting in a loss of planarity and hence shortening of the effective conjugation length. As for the polymers in the film state, both the UV and PL spectra of **BEH4P-PPV** and **BEH3P-PPV** are almost identical, whereas **BEH2P-PPV** displays a slight blue shift in its UV λ_{max} and a slight red shift in its PL λ_{max} . Again, this can be explained as

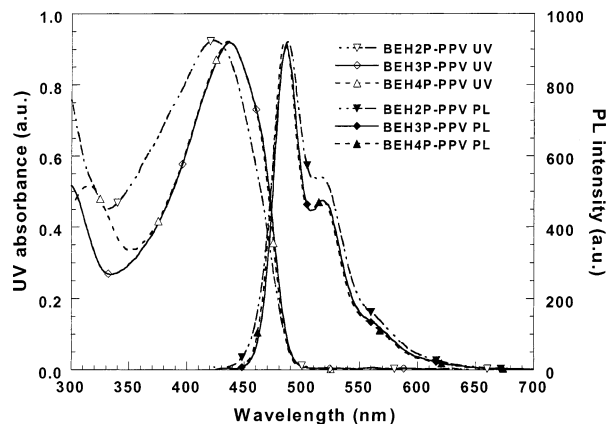


Figure 3. Absorption and fluorescence spectra of **BEH2P-PPV**, **BEH3P-PPV**, and **BEH4P-PPV** polymer solutions.

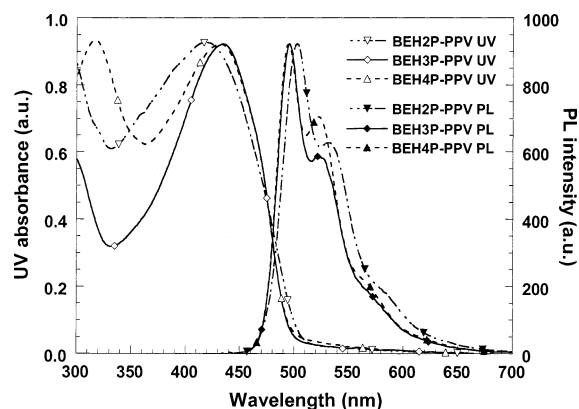


Figure 4. Absorption and fluorescence spectra of **BEH2P-PPV**, **BEH3P-PPV**, and **BEH4P-PPV** polymer films.

a result of the highly rigid structure of the polymers, leading to a loss in planarity between the phenyl rings. As such, a decrease in the conjugation length results and hence the blue shift in UV λ_{max} is observed as compared to the other polymers. On the other hand, the red shift in the PL λ_{max} of **BEH2P-PPV** in the film state, which is not observed when in the solution state, may be caused by the difference in geometries of the ground and excited states, which may be associated with the bulky phenyl ring in position-2 on the side group. In conjunction with the relaxation of vibronic energy bands, the difference in the minimum points of the potential curves of the ground and excited states on the configuration coordinates leads to further bathochromic shift between absorption and emission maxima. Generally, the geometric change in excited states will reduce the quantum efficiency due to nonradiative transition, which will be further discussed later. All the polymers exhibit well-defined side peaks in the PL spectra which is a result of vibronic coupling of excitons. The PL λ_{max} of the film samples show a slight red shift as compared to the solution samples. As seen from the values of the π - π^* band gap, the emission from the polymers falls in the region of green. The π - π^* band gaps were estimated from the edge absorptions of the film samples to be 2.47, 2.51, and 2.52 for **BEH2P-PPV**, **BEH3P-PPV**, and **BEH4P-PPV** respectively. The relative fluorescence quantum efficiency (η_{PL}) of the polymers was determined, in a dilute chloroform solution (1×10^{-6} M) using quinine sulfate (1×10^{-5} M) dissolved in 0.1 M H_2SO_4 as a standard, to be 0.66, 0.69, and 0.78 for **BEH2P-PPV**, **BEH3P-PPV**, and **BEH4P-PPV** respectively. There is a clear correlation between the

Table 2. Physical Properties of the Polymers

polymer	M_n/M_w ($\times 10^5$)	T_d ($^{\circ}\text{C}$) (onset)	UV λ_{max} , nm		band gap (eV)	PL λ_{max} , nm		η_{PL} solvent
			solvent	film		solvent	film	
BEH2P-PPV	3.6/7.7	314	423	418	2.47	487 (516)	502 (532)	0.66
BEH3P-PPV	1.3/3.1	339	437	434	2.51	486 (517)	496 (525)	0.69
BEH4P-PPV	5.7/9.2	300	(316) 436	(317) 432	2.52	485 (518)	494 (523)	0.78

Table 3. Electrochemical Data of the Polymers^a

polymer	p-doping (V)			n-doping (V)			energy levels (eV)		band gap (eV)
	$[E_{\text{onset}}]^{\text{ox}}$	E_a	E_c	$[E_{\text{onset}}]^{\text{red}}$	E_c	E_a	HOMO	LUMO	
BEH2P-PPV	0.90	1.34		-1.68	-2.06	-1.89	-5.30	-2.72	2.58
BEH3P-PPV	0.85	1.31		-1.60	-1.96	-1.86	-5.25	-2.80	2.45
BEH4P-PPV	0.86	1.18	1.17	-2.02	-2.34	-2.31	-5.26	-2.38	2.88

^a E_a and E_c represent the anodic and cathodic peak potentials, respectively.

η_{PL} and the polymer structure. The more well-separated the polymer chains, the higher the η_{PL} . As a result, the PL efficiency for **BEH4P-PPV** was observed to be the highest among the series of polymers. This may be due to the branched 2'-ethylhexyloxy side chains on opposite sides of the phenyl substituent, which effectively serve to separate the polymer chains from one another. The results are in accordance to those obtained for poly-(2-(2',5'-bis(2''-ethylhexyloxy)phenyl)-1,4-phenylenevinylene)¹⁷ and poly(3-(2,5-dioctylphenyl)-thiophene) (PDOPT). These polymers have demonstrated ~60% and 16% of PL efficiency in the film state, respectively. Compared to other PPVs or poly(3-alkylthiophenes), the improvement in efficiencies is very significant.^{39,40} The physical properties of the polymers are summarized in Table 2.

Electrochemical Properties. Cyclic voltammetry (CV) was employed to investigate the electrochemical behavior of the polymers as well as estimate the HOMO and LUMO energy levels of the materials. The polymer films deposited on a Pt electrode were scanned both positively and negatively separately in 0.10 M tetrabutylammonium perchlorate (Bu_4NClO_4) in anhydrous acetonitrile. In Figure 5, all the polymers showed reversible n-doping processes and except for **BEH4P-PPV**, which showed a partially reversible p-doping process, the other polymers showed irreversible p-doping processes. The onset potentials for oxidation were observed to be 0.90, 0.85, and 0.86 V (vs SCE) for **BEH2P-PPV**, **BEH3P-PPV**, and **BEH4P-PPV** respectively. On the other hand, the onset potentials for reduction were -1.68, -1.60, and -2.02 V (vs SCE), respectively. From the onset potentials of the oxidation and reduction processes, the band gaps of the polymers

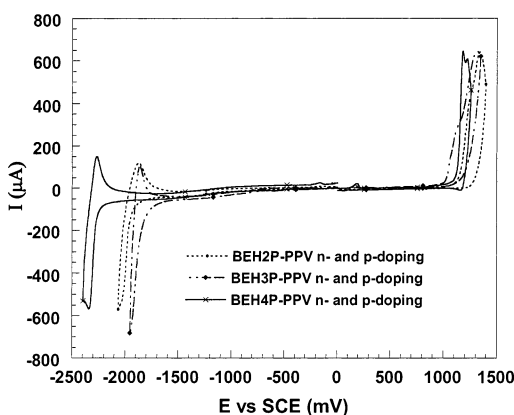


Figure 5. Cyclic voltammograms of **BEH2P-PPV**, **BEH3P-PPV**, and **BEH4P-PPV**.

were estimated to be 2.58, 2.45, and 2.88 eV for **BEH2P-PPV**, **BEH3P-PPV**, and **BEH4P-PPV** respectively. The values for **BEH2P-PPV** and **BEH3P-PPV** are quite close to those obtained by optical method while **BEH4P-PPV** shows higher energy gap. According to the equations,^{41,42} $\text{IP} = -([E_{\text{onset}}]^{\text{ox}} + 4.4)$ eV and $\text{EA} = -([E_{\text{onset}}]^{\text{red}} + 4.4)$ eV, where $[E_{\text{onset}}]^{\text{ox}}$ and $[E_{\text{onset}}]^{\text{red}}$ are the onset potentials for the oxidation and reduction of the polymer vs the reference electrode, the LUMO and HOMO of the polymers were estimated to be -2.72, -2.80, and -2.38 eV and -5.30, -5.25, and -5.26 eV for **BEH2P-PPV**, **BEH3P-PPV**, and **BEH4P-PPV** respectively. The electrochemical data of the polymers are summarized in Table 3. From Table 3, we find that the HOMO and LUMO energy levels of **BEH2P-PPV** and **BEH3P-PPV** are quite similar. As for **BEH4P-PPV**, its HOMO is close to the other two polymers while the LUMO is much higher. Therefore, the substitution pattern of the side chains will affect not only the polymerization process but also the energy levels of the polymers.

Electroluminescence Properties of LED Devices. Double layer LED devices based on the three polymers with the configuration of ITO/PEDOT/polymer/Ba/Al were fabricated. Poly(3,4-ethylenedioxythiophene) (PEDOT) doped with poly(styrenesulfonic acid) (PSS) (Batron-P 4083) with a thickness of 150 nm was used as the hole injection/transporting layer. A thin layer of Ba (5 nm) was employed as the cathode because it normally results in devices with longer lifetime due to its larger atomic size and mass as compared with Ca or Mg.⁴³ The Ba layer was coated with a 180 nm layer of Al. The thickness of the emissive layer is around 80 nm. The electroluminescence spectra are displayed in Figure 6, in which **BEH2P-PPV** and **BEH3P-PPV** follow the traces of their PL spectra, with peaks at 496, 488 nm and clear side peaks and shoulders at 529, 577 nm and 520, 567 nm, respectively. The similarity of the PL and EL spectra indicates that same excitations are involved in both cases. In contrast, the EL spectrum of **BEH4P-PPV** is different from its PL counterpart, which peaks at 525 nm with two side peaks at 490 and 566 nm. Compared with its PL spectrum, the change in relative intensities in vibronic structure indicates that aggregate emission is dominant in its EL process.^{44,45} The difference between the PL and EL spectra of **BEH4P-PPV** may be attributed to the following two reasons. First, the film for PL measurement was spin coated from xylene solution while that for LED device fabrication was prepared from chloroform solution. Different solvents may result in different amount of interchain

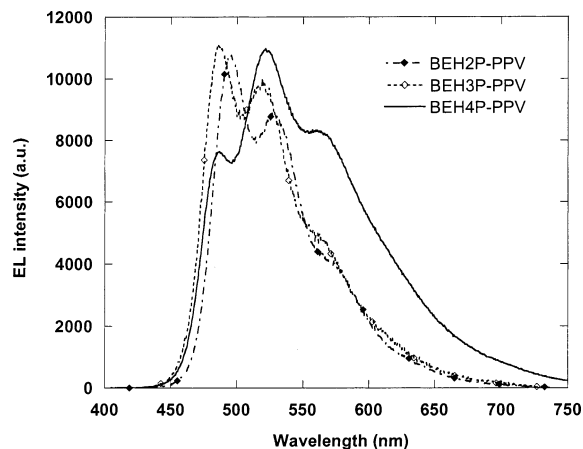


Figure 6. Electroluminescence spectra of the LEDs.

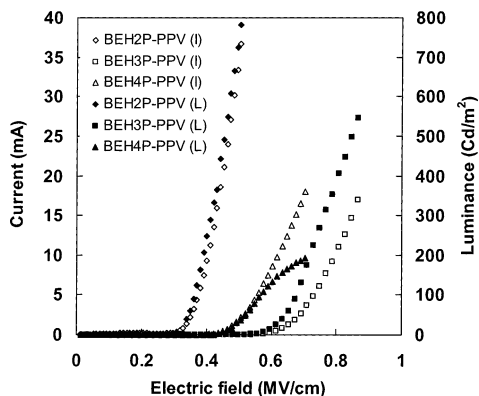


Figure 7. Current–voltage–luminance characteristics of ITO/PEDOT/polymer/Ba/Al devices: current, open markers; luminance, closed markers.

interactions, which will influence the emission characteristics.^{44,45} The second reason may be ascribed to the different emissive processes involved for PL and EL. An aggregate state in the polymer layer could serve as a trapping center since aggregates in the polymers are lower energy sites. For PL process, it only concerns exciton trapping, while during the EL process, there is an additional parallel process where the aggregates can trap the injected electrons and holes. If trapping of charges is significant compared with trapping of excitons, the difference between the PL and EL spectra will be notable. Because of concentration quenching in such sites, the emission efficiency is reduced. This behavior has also been observed in polyfluorene derivatives.³⁸

Figure 7 compares the I – V – L curves of the double layer devices. With an increase of forward electric field, both the current and luminance increase synchronically. Among the diodes, the EL performance of **BEH2P-PPV** shows the lowest turn-on electric field, followed by **BEH4P-PPV** and **BEH3P-PPV**. The turn-on electric fields are 0.30, 0.42, and 0.50 MV/cm, respectively. The lowest turn-on electric field observed in the **BEH2P-PPV** diode can be attributed to the lowest amount of tolane-bisbenzyl structural defects in **BEH2P-PPV**, which renders it the longest π electron conjugation and highest charge carrier mobility among the three polymers.³⁷ The required electric fields for 100 Cd/m² of emissive brightness are 0.36, 0.57, and 0.73 MV/cm. The maximum QEs are 0.37%, 0.66% and 0.25% for the diodes of **BEH2P-PPV**, **BEH3P-PPV**, and **BEH4P-PPV** respectively. We can find in Figure 8 that **BEH3P-PPV** holds the highest QE (0.5–0.7%),

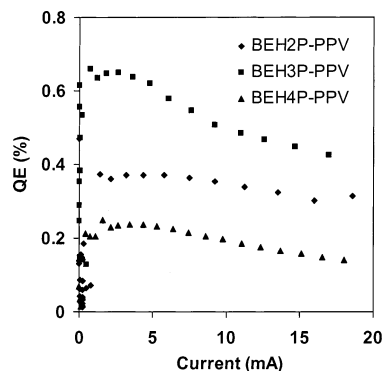


Figure 8. Dependence of quantum efficiency of the LED devices on current.

which is higher by factors of about 1.5 (**BEH2P-PPV**, ~0.4%) and 2.5–3.0 (**BEH4P-PPV**, ~0.2%). When we investigate the relationship between energy levels and devices performance, we find that the external quantum efficiency is mainly determined by the LUMOs of the polymers. Because the HOMO energy levels of the three polymers are much closer to the work function of PEDOT (5.2 eV), the barrier is very small for hole injection. On the other hand, the LUMO of the polymers are different from each other. The higher the LUMO of the polymer, the lower is the QE of the device. Therefore, holes are the major charge carriers in the devices and the rate of electron injection from the cathode determines the device efficiency among the investigated polymer diodes. Other possible factors which may affect the device efficiencies include interchain interactions in the film states. For example, aggregation emission in **BEH4P-PPV** is another key reason responsible for its lowest QE among the three polymer diodes. As for **BEH2P-PPV**, both the HOMO and LUMO energy levels are comparable to **BEH3P-PPV**; however, the quantum efficiency is lower. This might be ascribed to the geometric change in the excited state, as discussed before. Such a geometric change will generally lead to a bathochromic shift in emission spectrum, faster charge carrier mobility, and reduced quantum efficiency due to intersystem crossing. This may also be partially responsible for the lowest turn-on electric field for **BEH2P-PPV** diode.

Conclusion

A new series of dialkoxyphenyl-substituted PPV derivatives, **BEH2P-PPV**, **BEH3P-PPV**, and **BEH4P-PPV**, has been successfully synthesized using the Gilch method. The polymers possess desirable properties such as excellent solubility, high molecular weight, high PL efficiency, and good thermal stability. ¹H NMR investigation of the polymers indicates that substitution on the side chains which imposes strong steric hindrance is an effective approach to suppress the formation of structural defects during polymerization. In addition, solvents used for the Gilch route also play an important role with regards to the amount of TBB moieties in the polymers. Polar solvent resulting in a low amount of TBB may be ascribed to the accelerated anionic chain reaction during polymerization.

Double-layered LED devices with the configuration of ITO/PEDOT/polymer/Ba/Al revealed that **BEH2P-PPV** possesses the highest luminance, the lowest turn-on electric field, and a medium external quantum efficiency and is the most promising material among the

three polymers for polymer light-emitting devices. A longer operational lifetime is expected as a result of its negligible TBB defects along the polymer main chain.

References and Notes

- (1) Burroughes, J. H.; Bradley, D. D. C.; Brown, A. R.; Marks, R. N.; Mackay, K.; Friend, R. H.; Burn, P. L.; Holmes, A. B. *Nature (London)* **1990**, *347*, 539.
- (2) Friend, R. H.; Gymer, R. W.; Holmes, A. B.; Burroughes, J. H.; Marks, R. N.; Taliani, C.; Bradley, D. D. C.; Dos Santos, D. A.; Bredas, J. L.; Logdlund, M.; Salaneck, W. R. *Nature (London)* **1999**, *397*, 121.
- (3) Cao, Y.; Parker, I. D.; Yu, G.; Zhang, C.; Heeger, A. J. *Nature (London)* **1999**, *397*, 414.
- (4) Gustafsson, G.; Cao, Y.; Treacy, G. M.; Klavetter, F.; Colaneri, N.; Heeger, A. J. *Nature (London)* **1992**, *357*, 477.
- (5) Kraft, A.; Grimsdale, A. C.; Holmes, A. B. *Angew. Chem., Int. Ed.* **1998**, *37*, 402.
- (6) Mitschke, M.; Bauerle, P. *J. Mater. Chem.* **2000**, *10*, 1471.
- (7) Chung, S. J.; Kwon, K. Y.; Lee, S. W.; Jin, J. I.; Lee, C. H.; Lee, C. E.; Park, Y. *Adv. Mater.* **1998**, *10*, 1112.
- (8) Bao, Z.; Peng, Z.; Galvin, M. E.; Chandross, E. A. *Chem. Mater.* **1998**, *10*, 1201.
- (9) Chen, Z. K.; Meng, H.; Lai, Y. H.; Huang, W. *Macromolecules* **1999**, *32*, 4351.
- (10) Greenham, N. C.; Moratti, S. C.; Bradley, D. D. C.; Friend, R. H.; Burn, P. L.; Holmes, A. B. *Nature (London)* **1993**, *365*, 628.
- (11) Strukelj, M.; Papadimitrakopoulos, F.; Miller, T. M.; Rothberg, L. J. *Science* **1995**, *267*, 1969.
- (12) Conwell, E. *Trends Polym. Sci.* **1997**, *5*, 218.
- (13) Jenekhe, S. A. *Adv. Mater.* **1995**, *7*, 309.
- (14) Cornil, J.; Dos Santos, D. A.; Crispin, X.; Silbey, R.; Bredas, L. J. *J. Am. Chem. Soc.* **1998**, *120*, 1289.
- (15) Nguyen, T.-Q.; Martini, I. B.; Liu, J.; Schwartz, B. J. *J. Phys. Chem. B* **2000**, *104*, 237.
- (16) Peng, Z. H.; Zhang, J. H.; Xu, B. B. *Macromolecules* **1999**, *32*, 5162.
- (17) Johansson, D. M.; Theander, M.; Srdanov, G.; Yu, G.; Inganäs, O.; Andersson, M. R. *Macromolecules* **2001**, *34*, 3716.
- (18) Chen, Z. K.; Huang, W.; Wang, L. H.; Kang, E. T.; Chen, B. J.; Lee, C. S.; Lee, S. T. *Macromolecules* **2000**, *33*, 9015.
- (19) Sohn, B. H.; Kim, K. K.; Choi, D. S.; Kim, Y. K.; Jeoung, S. C.; Jin, J. I. *Macromolecules* **2002**, *35*, 2876.
- (20) Lee, S. H.; Jang, B. B.; Tsutsui, T. *Macromolecules* **2002**, *35*, 1356.
- (21) Jin, S. H.; Jang, M. S.; Suh, H. S.; Cho, H. N.; Lee, J. H.; Gal, Y. S. *Chem. Mater.* **2002**, *14*, 643.
- (22) Sarker, A. M.; Ding, L. M.; Lahti, P. M.; Karasz, F. E. *Macromolecules* **2002**, *35*, 223.
- (23) Becker, H.; Spreitzer, H.; Kreuder, W.; Kluge, E.; Schenk, H.; Parker, I.; Cao, Y. *Adv. Mater.* **2000**, *12*, 42.
- (24) Braun, D.; Heeger, A. *Appl. Phys. Lett.* **1991**, *58*, 1982.
- (25) Spreitzer, H.; Becker, H.; Kluge, E.; Kreuder, W.; Schenk, H.; Demandt, R.; Schöo, H. *Adv. Mater.* **1998**, *10*, 1340.
- (26) Becker, H.; Spreitzer, H.; Ibrom, K.; Kreuder, W. *Macromolecules* **1999**, *32*, 4925.
- (27) Pei, J.; Yu, W. L.; Huang, W.; Heeger, A. J. *Chem. Lett.* **1999**, *10*, 1123.
- (28) *Dictionary of Organic Compounds*, 5th ed.; Chapman and Hall: New York, 1982; Vol. 1, 530.
- (29) Wessling, R. A. *J. Polym. Sci. Symp.* **1985**, *72*, 55.
- (30) Denton, F. R., III; Sarker, F.; Lahti, P. M.; Garay, R. O.; Karasz, F. E. *J. Polym. Sci., Polym. Chem.* **1992**, *30*, 2233.
- (31) Burn, P. L.; Kraft, A.; Baigent, D. R. *J. Am. Chem. Soc.* **1993**, *115*, 10117.
- (32) Hsieh, B. R.; Yu, Y.; VanLaeken, A. C.; Lee, H. K. *Macromolecules* **1997**, *30*, 8094.
- (33) Neef, C. J.; Ferraris, J. P. *Macromolecules* **2000**, *33*, 2311.
- (34) Hontis, L.; Van Der Borgh, M.; Vanderzande, D.; Gelan, J. *Polymer* **1999**, *40*, 6615.
- (35) Chen, Z. K.; Pan, J. Q.; Xiao, Y.; Lee, N. H. S.; Chua, S. J.; Huang, W. *Thin Solid Films* **2000**, *363*, 98.
- (36) Young, R. N.; Quirk, R. P.; Fetter, L. J. *Adv. Polym. Sci.* **1984**, *7*, 56.
- (37) Remmers, M.; Neher, D.; Grüner, J.; Friend, R. H.; Gelinck, G. H.; Warman, J. M.; Quattrocchi, C.; dos Santos, D. A.; Brédas, J. L. *Macromolecules* **1996**, *29*, 7432.
- (38) List, E. J. W.; Guentner, R.; Scanducci de Freitas, P.; Scherf, U. *Adv. Mater.* **2002**, *14*, 374.
- (39) Andersson, M. R.; Berggren, M.; Thomas, O.; Hjertberg, T.; Inganäs, O.; Wennerström, O. *Synth. Met.* **1997**, *85*, 1383.
- (40) Andersson, M. R.; Thomas, O.; Mammo, W.; Svensson, M.; Theander, M.; Inganäs, O. *J. Mater. Chem.* **1999**, *9*, 1933.
- (41) de Leeuw, D. M.; Simenon, M. M. J.; Brown, A. R.; Einerhand, R. E. F. *Synth. Met.* **1997**, *87*, 53.
- (42) Cervini, R.; Li, X. C.; Spencer, G. W. C.; Holmes, A. B.; Moratti, S. C.; Friend, R. H. *Synth. Met.* **1997**, *84*, 359.
- (43) Cao, Y.; Yu, G.; Parker, I. D.; Heeger, A. J. *J. Appl. Phys.* **2000**, *88*, 3618.
- (44) Nguyen, T.-Q.; Martini, I. B.; Liu, J.; Schwartz, B. J. *J. Phys. Chem. B* **2000**, *104*, 237.
- (45) Chen, S.-H.; Su, A.-C.; Huang, Y.-F.; Su, C.-H.; Peng, G.-Y.; Chen, S.-A. *Macromolecules* **2002**, *35*, 4229.

MA021221N